

Diffusion-Trapping modelling of Hydrogen recycling in Tungsten under ELM like heat loads

K. Schmid*

Max-Planck-Institut für Plasmaphysik, EURATOM Association,
Boltzmannstraße 2, D-85748 Garching b. München Germany

Abstract

The recycling of D ions impinging onto a W divertor surface is a key input parameter into the power and momentum balance at the target boundary during SOL modeling. It is described by the ratio R of the flux of recombining D_2 molecules to the incident ion flux. In steady-state plasmas where the surface is in equilibrium with the incident flux R equals one due to particle conservation. However during transient events such as ELMs the evolution of R with time is not straight forward to predict. Therefore detailed diffusion-trapping calculations were performed taking into account the variations in power influx and particle energy during an ELM. They showed that in contrast to the naive expectation, that the ELM would deplete the surface and subsequently lead to "pumping" ($R \ll 1$) of the incident flux by the empty surface, $R \approx 1$ or even $R > 1$ occurs. This paper will first describe how the ELM was approximated in the 1D diffusion-trapping code and will then discuss the evolution of R during an ELM and in the inter ELM phase. Also an analytical picture of R will be developed which allows to qualitatively understand the evolution of R as calculated by the diffusion-trapping code.

1 Introduction

In current scrape off layer (SOL) models the recycling coefficient R , defined as the ratio of the re-emitted to the incident particle flux, is assumed to be essentially equal to one. This parameter defines the particle, energy and momentum balance at the divertor targets and thus also affects the upstream plasma parameters [1]. Since most SOL models deal with steady-state plasmas, $R = 1$ is a valid assumption for surfaces in equilibrium with the incident flux.

Under steady-state conditions the uptake of H into an initially empty W surface by implantation is initially dominated by filling the implantation range ($R \approx 0$) until the diffusion gradient towards the surface balances the incident flux ($R \approx 1$). At the same time also diffusion into the bulk starts but the diffusion gradient towards the bulk quickly flattens as the H profile propagates into depth. So once the implantation range has equilibrated the uptake of H into W is limited by the ever slowing bulk diffusion flux. Thus as long as the implantation range is in equilibrium $R \approx 1$ is true, since the uptake into the bulk is negligible compared to the out-diffusion at the surface.

From laboratory experiments [2] it is known that for tungsten (W) only a negligible fraction

*Corresponding Author

Tel: +49 89 3299 2228

Fax: +49 89 3299 2279

E-mail: Klaus.Schmid@ipp.mpg.de

of the incident flux is actually retained in the surface whereas the majority is released from the surface by out-diffusion and recombination. However under transient plasma conditions (e.g. ELMs) with strong variations in the incident particle flux and surface temperature the situation may be different since both diffusion and recombination exhibit a strong temperature dependence.

To investigate the time evolution of the recycling coefficient R under transient, ELM like, heat and particle loads the 1D diffusion-trapping code TESSIM [3] is used. The parameters for the diffusion-trapping part were chosen according to typical literature values for the diffusion coefficient and de-trapping energies of H in W [2]. The calculations include the time evolution of the power load $\Phi^{In}(\frac{W}{m^2})$, particle flux $\Gamma^{Ion}(m^{-2})$ and particle energy $E^{Ion}(eV)$. The ELM is approximated as a gauss shaped pulse in Φ^{In} , Γ^{Ion} and E^{Ion} with a FWHM τ . The surface temperature is calculated as function of time and depth corresponding to the time varying power flux $\Phi^{In}(t)$.

The calculations showed that $R \approx 1$ is essentially always a good choice for typical divertor particle fluxes, even under conditions where the target surface is heavily depleted by out-diffusion due to a temperature excursion. The reason for this unexpected result is that re-equilibrating the implantation range to reach $R \approx 1$ happens instantaneously for typical divertor particle fluxes. $R \ll 1$ can only be reached for extremely low influxes which is typically not the case during a transient event.

The paper will first describe the modeling assumptions that were applied in TESSIM. Then the calculations results will be presented together with an analytical model for the H uptake into W which allows to qualitatively understand the diffusion-trapping code calculation results.

2 Model Description

2.1 The Diffusion-Trapping model in TESSIM

The commonly accepted picture of hydrogen H in metals such as Fe [4] or W [3] (endothermal solution of H) is that H is stored partially as solute in tetrahedral or octahedral sites and partially in defects. In the latter it is considered trapped and immobile until it de-traps into a solute site and continues to diffuse according to Fick's second law. The traps have fixed binding energies, different for each trap type and do not depend on the occupancy level of hydrogen in the trap [5, 4, 3]. The de-trapping step is thermally activated and is usually described by an Arrhenius type expression. This picture is very successful in describing experiments where hydrogen is loaded into the material by ion implantation and is subsequently degassed in a Thermal Desorption Experiment (TDS) [3, 2]. This model has been implemented in different codes where TMAP7 [5] is probably the most popular. The code TESSIM used in this work applies the same basic equations but is implemented in Mathematica giving it unprecedented flexibility in making changes to the different parts of the model without performance degradation.

The governing equations in TESSIM that describe the solute diffusive transport and the interaction with trap sites is given in eq. 1. It describes the time evolution of the solute concentration as the sum of diffusion, a distributed bulk source (implantation) and loss/gain to/from traps.

$$\frac{\partial C_{SOL}(x,t)}{\partial t} = D(T(x,t)) \frac{\partial^2 C_{SOL}(x,t)}{\partial^2 t} + S(x,t) - \sum_{i=0}^{N_{Trap}-1} \frac{\partial C_{Trap,i}(x,t)}{\partial t} \quad (1)$$

$$\frac{\partial C_{Trap,i}(x,t)}{\partial t} = \alpha(T(x,t))C_{SOL}(x,t) (\eta_i(x,t) - C_{Trap,i}(x,t)) - \beta_i(T(x,t))C_{Trap,i}(x,t)$$

$C_{SOL}(x,t)$ = Solute concentration at depth x and time t
 $C_{Trap,i}(x,t)$ = Concentration of H trapped in trap type i
 $D(T(x,t))$ = Solute diffusion coefficient ($\frac{m^2}{s}$) as function of temperature T
 $\alpha(T(x,t))$ = Trapping rate (s^{-1})
 $\beta_i(T(x,t))$ = De-trapping rate from trap type i (s^{-1})
 $S(x,t)$ = Volume source of H due to implantation(s^{-1})

The solute diffusion coefficient used in this work is that from [6] which is commonly [3, 2] used in diffusion-trapping modeling. The trapping rate α is chosen as the average jump rate over one lattice distance a_0 (from a solute site into an adjacent trap site) based on the current diffusion coefficient as: $\alpha = \frac{D}{a_0^2}$ by invoking the Einstein relation. The de-trapping rate β_i from trap-type i is described as an Arrhenius process with trap-type-dependent frequency factor $\nu_i (s^{-1})$ and activation energy $E_i^{TS} (eV)$ as: $\beta_i = \nu_i \exp\left(\frac{E_i^{TS}}{K_B T}\right)$. In this work based, on experience with lab experiments [3, 2], two types of traps characterized by a particular ν_i and E_i^{TS} were used. The near-surface trap site concentration profile in W is known to evolve with time [3, 2]. However this evolution is not continuous, but saturates at fluences that can be reached in laboratory experiments. Therefore, for the high fluxes and fluences occurring at the strike point in a current fusion experiment this time evolution was neglected and the calculations were performed starting with a typical equilibrium distribution of trap sites derived from depth profile in literature[3, 2]. This choice of the trap concentration profiles together with the values of ν_i and E_i^{TS} are shown in Fig. 1.

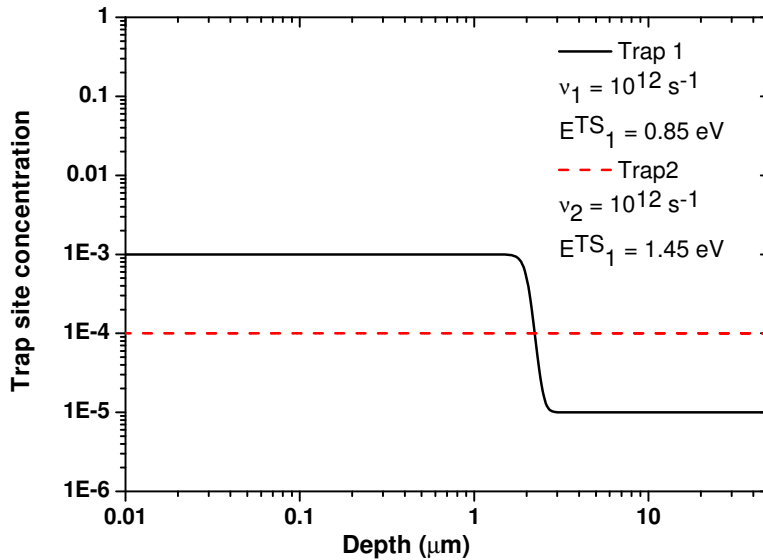


Figure 1: Constant trap concentration profiles and trap parameters used in the calculation

It should be noted that at the high temperatures $400 \leq T \leq 800\text{K}$ considered here the detailed choices of the trap profile and trap parameters are of little importance: For the typical W de-trapping energies in the order of 0.8 to 1.45eV $\alpha(T) \leq \beta_i(T)$ and thus all traps are only partially filled and therefore do not heavily affect the transport of H. Also for W in this temperature range the trap sites do not anneal as was concluded from TEM imaging in [7] where no change in the dislocation density was found up to 1200K. Therefore, the choice of a constant trap concentration profile seems justified.

Apart from the trap profiles and trap parameters another key input into the model are the boundary conditions at the plasma wetted ($x = 0$) and far side ($x = X_{Max}$) surfaces. In W the release from the surface happens via recombination of two H atoms to a H_2 molecule which then desorbs from the surface. However, this recombination step is typically not the rate limiting step for the release of H [3]. The release is typically limited by the diffusion of H from the bulk to the surface. Therefore, the simplest choice for the boundary condition is a diffusion limited boundary condition which translate to a Dirichlet boundary condition $C_{SOL}(x = 0 \text{ or } x = X_{Max}, t) \equiv 0$.

2.2 Modeling the ELM temperature and particle spectrum excursion

As described in the introduction the ELM modifies the following parameters in the diffusion-trapping model: The temperature $T(x, t)$ as function of time and depth due the increase in the incident power flux $\Phi^{In}(\frac{W}{m^2})$. The incident ion flux $\Gamma^{Ion}(m^{-2}s^{-1})$ and the ion energy E^{Ion} are increased. According to Ref. [8] E^{Ion} is a combination of the hot ion temperature in the ELM (similar to values found in the pedestal region of the fusion plasma) plus the acceleration by the sheath, thus reaching ion energies of the order of 1keV. This increase in Γ^{Ion} and E^{Ion} manifests itself in volume source term $S(x, t)(s^{-1})$ in the diffusion-trapping model by changing the reflected fraction $R(E^{Ion})$ and the source distribution $\chi(x, E^{Ion})(m^2)$. In TESSIM for ion implantation $S(x, t)$ is approximated by the product of $(1 - R(E^{Ion}))\Gamma^{Ion}$ with a range distribution function $\chi(x, E^{Ion})$. For $\chi(x, E^{Ion})$ a gauss function is used. It is centered around the mean projected range of the ions $R_P(E^{Ion})$ and has a width derived from the ion range straggle $\Delta R_P(E^{Ion})$. The expression for $S(x, t)$ is shown in eq. 2.

$$\begin{aligned}
 S(x, t) &= (1 - R(t))\Gamma^{Ion}(t)\chi(x, t) & (2) \\
 \chi(x, t) &= \frac{\sqrt{2/\pi}}{\rho\Delta R_P(t) \left(1 + \text{Erf} \left(\frac{R_P(t)}{\sqrt{2}\Delta R_P(t)}\right)\right)} \exp\left(\frac{-(R_P(t) - x)^2}{2\Delta R_P(t)^2}\right) \\
 \rho &= \text{Number density of the host lattice W } 6 \times 10^{28}(m^{-3}) \\
 \chi(x, t) &= \chi(x, E^{Ion}(t)) \\
 R(t) &= R(E^{Ion}(t)) = \text{Reflection coefficient} \\
 R_P(t) &= R_P(E^{Ion}(t)) \\
 \Delta R_P(t) &= \Delta R_P(E^{Ion}(t))
 \end{aligned}$$

The range parameters R_P and ΔR_P are taken from trim calculations using the program SDTrim.SP [9, 10, 11].

The increase with time t of $\Phi^{In}(t)$, $\Gamma^{Ion}(t)$ and $E^{Ion}(t)$ due to the ELM is approximated as a gauss shaped pulse $\Omega(t)$ with width τ that is added to the inter-ELM value of these parameters. For the Source $S(x, t)$ the resulting profile at ELM and inter-ELM times is depicted in Fig. 2 showing the strong source increase during the ELM.

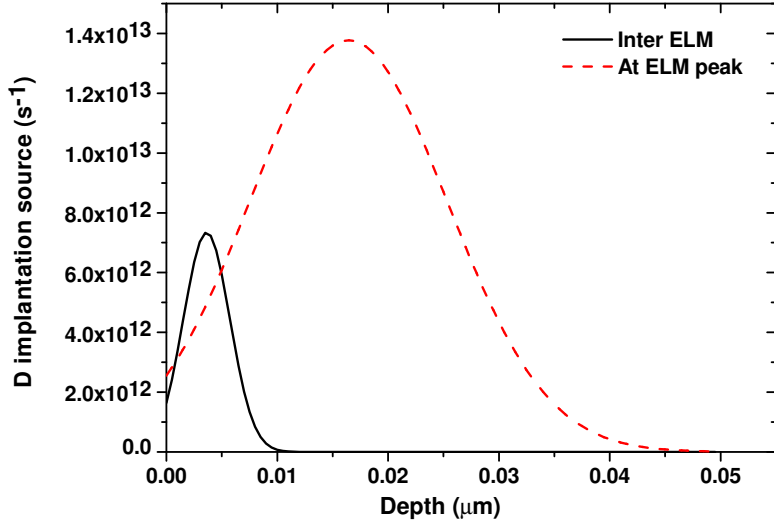


Figure 2: Comparison of the H particle source depth distribution $S(x,t)$ during and at the peak of the ELM

Not only does the magnitude of the source increase during the ELM but also its average depth increases resulting in slower out-diffusion of the implanted species and thus more efficient and faster uptake of H into W.

To correctly include the temperature evolution during the ELM the change in the temperature field $T(x,t)$ due to $\Phi^{In}(t)$ is calculated by solving the heat transport equation. On the plasma wetted side ($x = 0$) a Neumann boundary condition based on the difference between the power influx $\Phi^{In}(t)$ and the power radiated from the surface applying the Steffan-Boltzmann law: $\Phi^{Rad} = \epsilon\sigma T^4$. For W a spectral emissivity $\epsilon \approx 0.4$ [12] is used. On the far side ($x = x_{Max}$) a constant temperature Dirichlet boundary condition with $T = 473K$ was applied. The resulting expressions are summarized in eq. 3.

$$\begin{aligned}
 \frac{\partial T(x,t)}{\partial t} &= \zeta \frac{\partial^2 T(x,t)}{\partial x^2} & (3) \\
 \frac{\partial T(x,t)}{\partial x} \Big|_{x=0} &= -\frac{\Phi^{In} - \Phi^{Rad}}{\lambda} \\
 T(x_{Max}, t) &= \text{Const} = 473K \\
 \zeta &= \text{Const.} = \text{Heat diffusivity in W } (6.8 \times 10^{-5} \frac{\text{m}^2}{\text{s}}) \\
 \lambda &= \text{Const.} = \text{Thermal conductivity in W } (173 \frac{\text{W}}{\text{m K}})
 \end{aligned}$$

The actual time evolution of Φ^{In} used for the calculations and the resulting $T(x,t)$ are depicted in Fig. 3. After a ramp up the impact of 7 ELM like events in total is simulated yielding the temperature evolution plotted in Fig. 3. The width τ of the gauss peak in "ELM like" power excursion was chosen to be 4 ms following recent results from [13].

The temperature was calculated as function of time and depth where the thickness ($x_{Max} = 0.1m$) of the W sample was chosen such as to mimic what is found in current day inertially cooled fusion experiments such as JET with the iter like wall (JET-ILW): The base surface temperature of the inertially cooled W target surface increases and each "ELM like" event

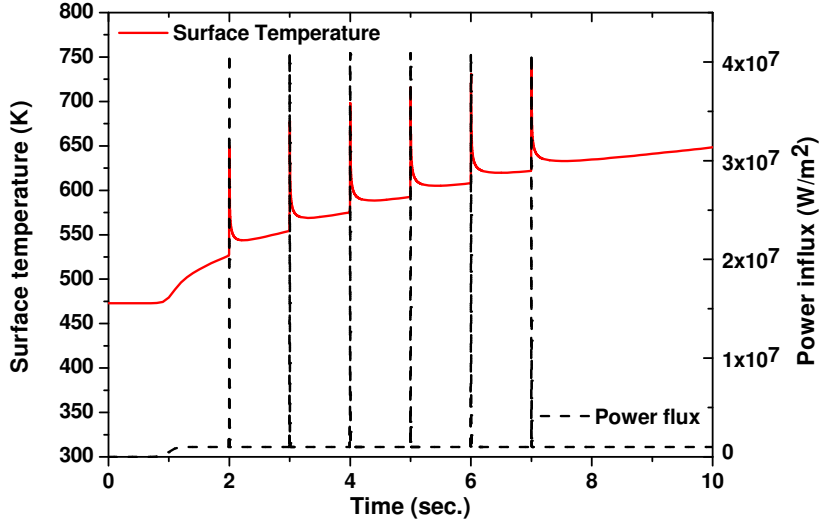


Figure 3: Comparison of the H particle source depth distribution $S(x, t)$ during and at the peak of the ELM

results in an additional temperature spike with a relative temperature rise of $\approx 100\text{K}$. The temperature gradient in depth both during and inter ELM is negligible within the diffusion depth reached by the diffusing hydrogen, none the less it is fully included in the diffusion-trapping calculations.

Equivalently to the power flux Φ^{In} also $\Gamma^{Ion}(t)$ and $E^{Ion}(t)$ are varied in time between base value and a maximum peak value during the ELM. $\Gamma^{Ion}(t)$ was varied between 1×10^{23} and 6×10^{23} D-ions $m^{-2}s^{-1}$ thus being a reasonable representation of the ion flux evolution during ELM's on the JET-ILW target. $E^{Ion}(t)$ was varied between an inter ELM base value of 50eV to a peak ELM value of 1000eV. As described above the variation of $E^{Ion}(t)$ entered the diffusion-trapping calculations via the derived parameters $R_P(E^{Ion}(t))$ and $\Delta R_P(E^{Ion}(t))$ in eq. 2.

Of course the above is not an accurate model of an ELM, but should w.r.t hydrogen uptake and release closely mimic the dominating effects of ELM such power and particle loads in current day fusion experiments: Temperature, flux and particle energy excursions on a ms time scale with a repetition frequency in the Hz range.

3 Results and Discussion

The model and input choices described in section 2 allow to calculate the time evolution of the concentration of trapped $C_{Trap,i}$ and solute hydrogen in the W surface exposed to "ELM-like events". From this output the out-diffusion flux $\Gamma^{OUT}(m^{-2}s^{-1})$ at the plasma wetted surface can be calculated invoking Fick's first law and from that R can be calculated as summarized in eq. 4.

$$\Gamma^{OUT}(t) = -D(T(t))\rho \frac{\partial C_{SOL}(x, t)}{\partial x} \Big|_{x=0} \quad (4)$$

$$R = \frac{\Gamma^{OUT}(t)}{\Gamma^{Ion}(t)}$$

The resulting depth profiles are shown in Fig. 4 for three times (Before 1.9 sec, at the

peak 2.0 sec. and after/inter ELM 2.1 sec.) around a single ELM like event. In the total (\equiv Solute + Trapped) profile one can see that despite the high temperature during the ELM, which leads to strong de-trapping, only very little depletion of the surface occurs due to the short time scale of the temperature excursion. Also the depletion is partially compensated by the increase in $S(x, t)$. In the solute profile one can see that the gradient towards the surface, which determines the out-diffusion of retained H, immediately steepens as the ELM hits. i.e. it follows increase in $S(x, t)$ already hinting towards little variation in R during the ELM.

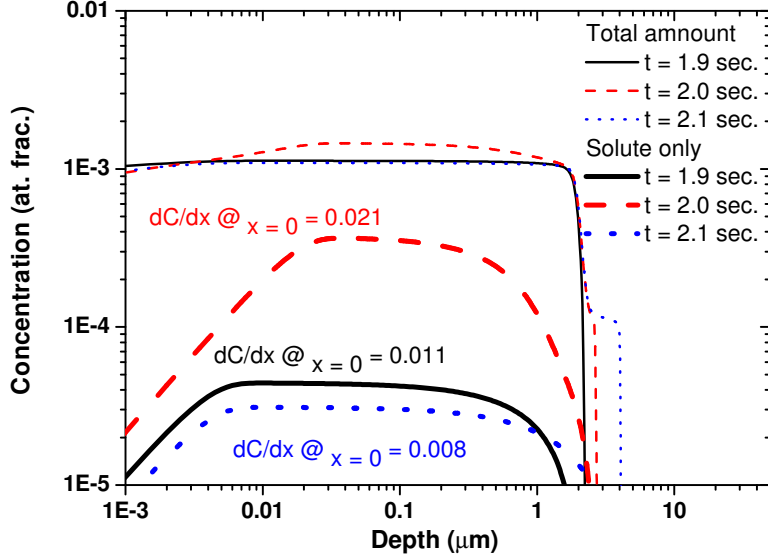


Figure 4: Total and Solute only depth profiles of H in W around the time of the first ELM-like event at $t = 2$ sec. Also noted are solute concentration gradients at the surface that drive out-diffusion.

The resulting variation in R around a single ELM-like event at $t = 6$ sec. and in between two ELM-like events at 6 and 7 sec. are shown in Fig. 5.

During a single ELM-like event R first decreases to $R \approx 0.976$ as $S(x, t)$ steeply increases then after the ELM as $S(x, t)$ decreases to base level R increases above 1 as the surface re-equilibrates with the now lower $S(x, t)$. At later times in the inter-ELM phase R does decrease to $R \approx 0.999$ but still essentially $R \approx 1$ holds throughout the ELM-like event. So counter intuitively $R \approx 1$ holds despite the depletion in the retained amount of H. Immediately after the ELM-like event it even increases to values > 1 . So no pumping of the incident flux occurs during the inter-ELM phase.

The influence of ELM-like events on the total retention is shown in Fig. 6. There a comparison of the total retained amount as function of time of a calculation with base load only and with ELM-like events is shown. For the parameters in this simulations the total retention in the presence of ELM-like events is slightly reduced. However while the ELM-like events slightly deplete the near surface region they drive the H deeper into the W bulk (see Fig. 4) thus increasing the depth reached by permeation.

The results presented here show the impact of ELM-like events for parameters typical for current day fusion devices. However future devices will have higher ELM power and thus higher surface temperature excursions which will lead to strong depletion of the surface. However the result of $R \approx 1$ still holds, since even then the solute quickly adapts to changes in $S(x, t)$

balancing influx and out-flux of H. The filling of W with H is diffusion limited so even a fully depleted W surface can only be filled at a limited rate thus excessive pumping of the incident flux is not expected even in future machines. The following section presents a simple analytical picture that helps to understand this behavior.

3.1 Analytical model

The result from the diffusion-trapping calculations that essentially $R \approx 1$ always holds, even under transients, is at first hard to understand. Therefore a simple analytical picture will now be developed that qualitatively shows the reasons for this result.

In Fig.7 the physical picture behind the analytical model is depicted: The depth profile evolving during the loading of W with H is approximated by a particle source located at the depth of the mean implantation range R_P and two solute gradients: The first steepest gradient from R_P towards the surface and the second from R_P towards a moving adsorbing boundary condition at location $R_D(t)$. This adsorbing boundary is due to trapping, which leads to depletion of the solute population at locations where the solute and the trapped population are not in equilibrium: The traps have to be saturated/equilibrated before the solute profile can continue to larger depths. These two gradients balance the ion influx Γ^{Ion} at R_P by diffusion fluxes (Γ^{Surf} towards the surface and Γ^{Bulk} towards the bulk). This allows to setup the flux balance equation at $x = R_P$ shown in eq. 5.

$$\begin{aligned}
0 &= \Gamma^{Ion} + \Gamma^{Surf} + \Gamma^{Bulk} & (5) \\
\Gamma^{Bulk} &= -D(T)\rho \frac{0 - C_{Max}(t)}{R_D(t)} \\
\Gamma^{Surf} &= -D(T)\rho \frac{C_{Max}(t) - 0}{R_P} \\
-D(T) &= \text{Solute diffusion coefficient} \\
\rho &= \text{Host lattice (W) number density (m}^{-3}\text{)} \\
C_{Max}(t) &= \text{Maximum solute concentration occurring at } x = R_P
\end{aligned}$$

The position $R_D(t)$ of the moving adsorbing boundary moves into depth as the traps in the bulk are filled continuously flattening the bulk gradient and reducing Γ^{Bulk} . This means that $C_{Max}(t)$ needs to increase to still balance the fluxes.

At $R_D(t)$ the traps are filled at a rate limited by Γ^{Bulk} therefore the velocity at which R_D moves is given by $\frac{\Gamma^{Bulk}}{C^{Trap}(T)\rho}$ and thus $R_D(t) = \frac{\Gamma^{Bulk}}{C^{Trap}(T)\rho}t$. $C^{Trap}(T)$ thereby denotes the concentration of traps that need to be filled before the solute can propagate further. Inserting this expression for $R_D(t)$ into eq. 5 yields the following result in eq. 6 for $C_{Max}(t)$

$$C_{Max}(t) = \frac{\left(C^{Trap}(T)\rho R_P + 2 * \Gamma^{Ion}t - \sqrt{C^{Trap}(T)\rho R_P \sqrt{C^{Trap}(T)\rho R_P + 4 * \Gamma^{Ion}t}} \right)}{2D(T)\rho t} \quad (6)$$

The recycling coefficient R is given by the ratio of the incident flux Γ^{Ion} to the out diffusion flux Γ^{Surf} and can thus be calculated using eq. 6 in the expression for Γ^{Surf} in eq. 5. The resulting expression for R(T) is given in eq. 7 together with the two limiting cases $t \rightarrow 0$ and $t \rightarrow \infty$ which allow to understand the two distinct time scales on which R(t) evolves.

$$\begin{aligned}
R(t) &= 1 + \frac{C^{Trap}(T)\rho R_P}{2\Gamma^{Ion}t} \left(1 - \sqrt{1 + \frac{4\Gamma^{Ion}t}{C^{Trap}(T)\rho R_P}} \right) \\
R(t \rightarrow \infty) &= 1 \\
R(t \rightarrow 0) &= \frac{2\Gamma^{Ion}t}{C^{Trap}(T)\rho R_P} t
\end{aligned} \tag{7}$$

For long times when the entire bulk is saturated R has to reach its equilibrium value of 1. This is the slow component of $R(t)$. For short time scales R is determined by the rate at which the near surface traps (at location $x \leq R_P$) are filled, this denotes the fast component of $R(t)$. At fixed temperature the dominating parameter in $R(t)$ is the ion flux. In Fig. 8 the time evolution of R is plotted for different ion flux values. It clearly shows the two time scales: A very fast initial rise to $R \approx 1$ followed by a slow increase until actually $R = 1$ is reached.

The fast component in eq. 7 takes values in the order of μsec for typical divertor fluxes in the range of $10^{23} m^{-2} s^{-1}$ and trap concentrations in W in the range of 10^3 . Therefore the recycling coefficient can easily follow the ion flux excursions during and ELM which occurs on the ms scale.

4 Summary

The evolution of the recycling coefficient R , defined as the ratio of the diffusive out-flux to the ion influx, is calculated using a diffusion-trapping code for W exposed to a particle influx with ELM-like excursion in power and particle flux. The parameters for the calculation were thereby chosen such as to mimic the conditions at the W targets of current fusion experiments like JET-ILW. The calculations show that despite slight depletion of the surface from H during the ELM, $R \approx 1$ always holds. There is no pumping ($\Leftrightarrow R \ll 1$) of the incident flux during the inter-ELM phase, on the contrary as the surface re-equilibrates with the lower flux $R > 1$ occurs for short time periods in between ELM-like events. An analytical model for the filling of W with H was developed that allows to understand this behavior. It shows that the filling of W by H is diffusion limited and happens on two time scales: A short one during which the ion implantation range is saturated with H which for typical divertor conditions is in the order of μs and a long time scale during which the bulk is filled with H . It is the short μs time scale that determines the variation of R for low fill levels which explains why $R \approx 1$ also holds under particle source excursions on the ms time scale. This principal, qualitative picture also holds for higher power and particle fluxes that can lead to more severe depletion of the W surface from H during an ELM event as expected in future machines. So $R \approx 1$ seems to be a general finding for fusion experiment divertor conditions under ELM-like loads.

References

- [1] M. Wischmeier, A. Kallenbach, A.V. Chankin, D.P. Coster, T. Eich, A. Herrmann, H.W. Müller, and ASDEX Upgrade Team. *Journal of Nuclear Materials*, 363:448, 2007.
- [2] O. V. Ogorodnikova, J. Roth, and M. Mayer. *J. Appl. Phys*, 103:34902, 2008.
- [3] K. Schmid, V. Rieger, and A. Manhard. *Journal of Nuclear Materials*, 426:247, 2012.
- [4] A. H. M. Krom and A. Bakker. *METALLURGICAL AND MATERIALS TRANSACTIONS B*, 31B:1475, 2000.

- [5] G. R. Longhurst and J. Ambrosek. *Fusion Science and Technology*, 48:468, 2005.
- [6] R. Frauenfelder. *J. Vac. Sci. Technol.*, 6(3):388, 1969.
- [7] A. Manhard, K. Schmid, M. Balden, and W. Jacob. *J. Nucl. Mater.*, 415:632, 2011.
- [8] R.A. Pitts, W. Fundamenski, S.K. Erents, Y. Andrew, A. Loarte, C. Silva, and JET-EFDA contributors. *Nuclear Fusion*, 46:82, 2006.
- [9] W. Eckstein, R. Dohmen, A. Mutzke, and R. Schneider. *Report IPP, Garching*, 12/3, 2007.
- [10] J.P. Biersack and W. Eckstein. *Appl. Phys. A*, 34:73, 1984.
- [11] W. Eckstein. *Computer Simulation of Ion-Solid Interactions*. Springer Verlag, 1991.
- [12] L.R. David. *CRC-Handbook of Chemistry & Physics, 75th Ed.* CRC, 1994.
- [13] E. de la Luna, P. Lomas, S. Saarelma, I. Nunes, L. Frassinetti, S. Bresinsek, and et al. Comparative study of high triangularity h-mode plasma performance in jet with be/w wall and cfc wall. *IAEA Conference St. Petersburg 2014, submitted to Nuclear Fusion*.

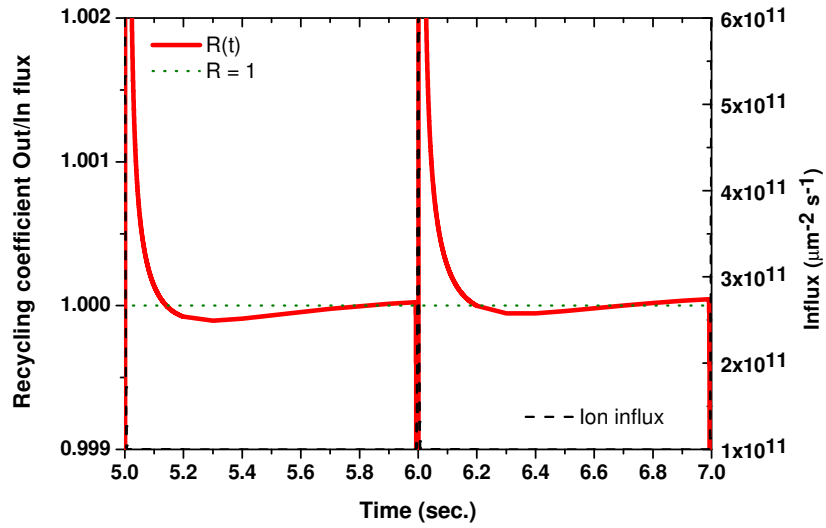
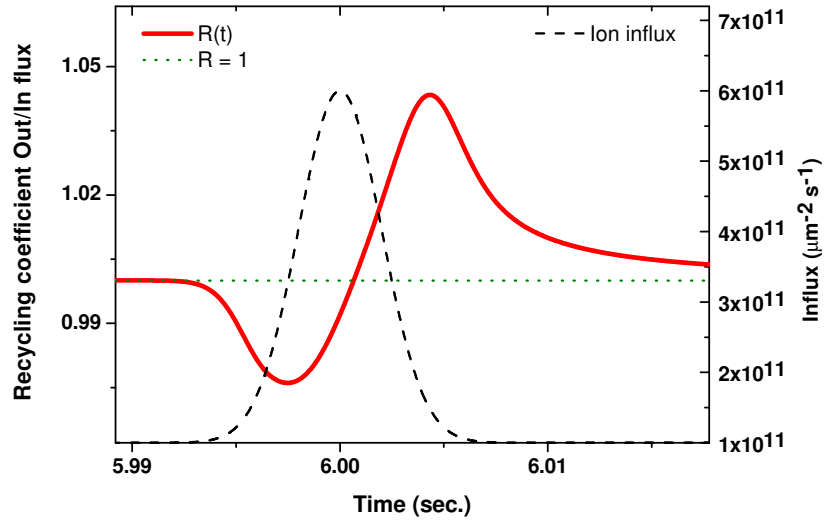


Figure 5: Zoom into the time evolution of R for a single ELM-like event at $t = 6$ sec. and for two ELM-like events at $t = 6$ and 7 sec.

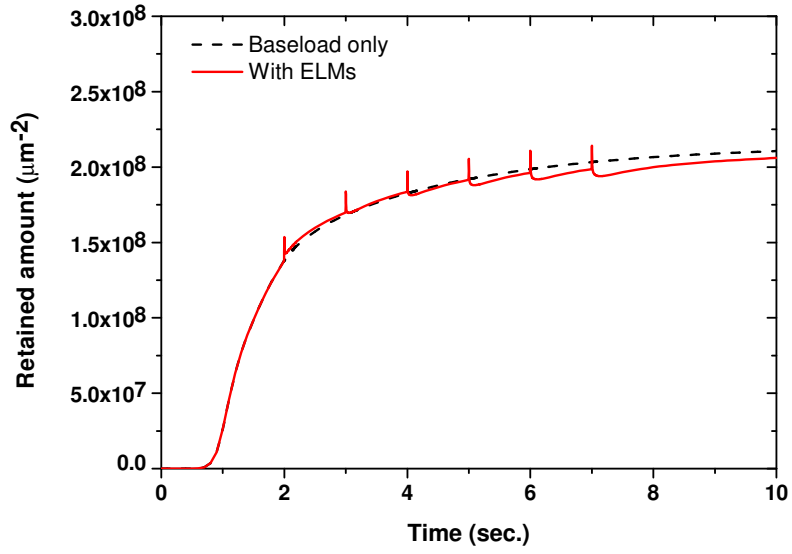


Figure 6: Total retention as function of time with and without ELM-like events.

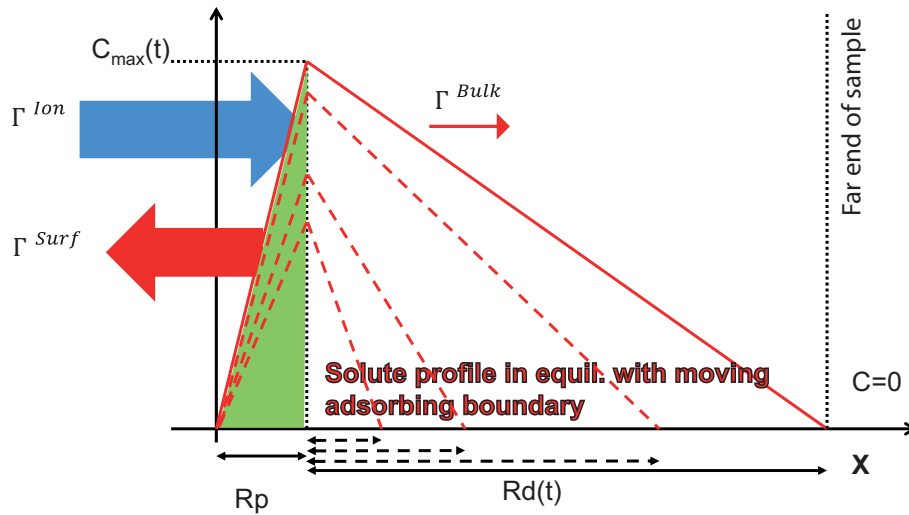


Figure 7: Sketch of the modeling assumptions entering the analytical picture of H loading of W

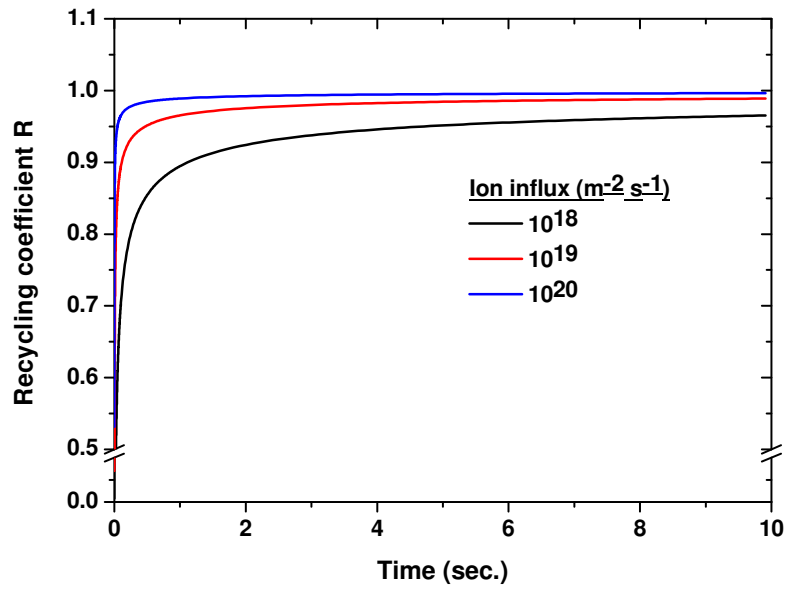


Figure 8: Time evolution of the recycling coefficient according to the analytical model. Showing fast initial increase of $R \approx 1$ followed by the slow increase towards $R = 1$